Short-Term Convective Mode Evolution along Synoptic Boundaries

GREG L. DIAL, JONATHAN P. RACY, AND RICHARD L. THOMPSON

NOAA/NWS/Storm Prediction Center, Norman, Oklahoma

(Manuscript received 9 June 2009, in final form 22 March 2010)

ABSTRACT

This paper investigates the relationships between short-term convective mode evolution, the orientations of vertical shear and mean wind vectors with respect to the initiating synoptic boundary, the motion of the boundary, and the role of forcing for ascent. The dominant mode of storms (linear, mixed mode, and discrete) was noted 3 h after convective initiation along cold fronts, drylines, or prefrontal troughs. Various shear and mean wind vector orientations relative to the boundary were calculated near the time of initiation. Results indicate a statistical correlation between storm mode at 3 h, the normal components of cloud-layer and deep-layer shear vectors, the boundary-relative mean cloud-layer wind vector, and the type of initiating boundary. Thunderstorms, most of which were initially discrete, tended to evolve more quickly into lines or mixed modes when the normal components of the shear vectors and boundary-relative mean cloud-layer wind vectors were small. There was a tendency for storms to remain discrete for larger normal shear and mean wind components. Smaller normal components of mean cloud-layer wind were associated with a greater likelihood that storms would remain within the zone of linear forcing along the boundary for longer time periods, thereby increasing the potential for upscale linear growth. The residence time of storms along the boundary is also dependent on the speed of the boundary. It was found that the boundary-relative normal component of the mean cloud-layer wind better discriminates between mode types than does simply the ground-relative normal component. The influence of mesoscale forcing for ascent and type of boundary on mode evolution was also investigated. As expected, it was found that the magnitude and nature of the forcing play a role in how storms evolve. For instance, strong linear low-level convergence often contributes to rapid upscale linear growth, especially if the boundary motion relative to the mean cloud-layer wind prevents storms from moving away from the boundary shortly after initiation. In summary, results from this study indicate that, for storms initiated along a synoptic boundary, convective mode evolution is modulated primarily by the residence time of storms within the zone of linear forcing, the nature and magnitude of linear forcing, and secondarily by the normal component of the cloud-layer shear.

1. Introduction and background

One of the more unique challenges facing severe weather forecasters is the correct anticipation of convective initiation and the subsequent mode and evolution of thunderstorms. Observational studies (Thompson et al. 2007; Gallus et al. 2008) indicate that tornadoes are more likely to occur with persistent discrete cells given a favorably sheared environment. Though tornadoes are observed with some quasi-linear convective systems (Przybylinski 1995; Funk et al. 1999; Przybylinski et al. 2000; Atkins et al. 2004; Trapp et al. 2005), damaging wind gusts are the more frequent severe weather threat with linear convective modes. Therefore, a more skillful forecast of severe weather hazards would likely result from a correct prediction of the organization and evolution of storms.

Historically, thermal buoyancy and vertical shear have been shown to be useful discriminators between supercell and nonsupercell thunderstorm modes (Weisman and Klemp 1982; 1984). Through three-dimensional idealized cloud model simulations, Weisman and Klemp showed that a spectrum of storm structures evolved when the thermal buoyancy and vertical shear were varied over an array of environmental conditions. The ratio of buoyancy to vertical wind shear, in the form of a nondimensional bulk Richardson number, was found to be useful in determining basic storm structures. Later observational studies using proximity soundings (Rasmussen and Blanchard 1998; Thompson et al. 2003; Craven and Brooks 2004) supported the findings of the Weisman and Klemp numerical simulations in using measures of vertical shear

Corresponding author address: Greg Dial, Storm Prediction Center, 120 David L. Boren Blvd., Norman, OK 73072.
E-mail: greg.dial@noaa.gov

DOI: 10.1175/2010WAF2222315.1

and buoyancy to discriminate between supercell and nonsupercell thunderstorms.

Other environmental characteristics, however, appear to play a substantial role in determining how thunderstorms evolve once they have become established. Attempts to address this problem have been limited and focused primarily on idealized numerical simulations. Observational studies by Bluestein and Jain (1985), Bluestein et al. (1987), and Bluestein and Parker (1993) investigated parameters believed to influence the nature and evolution of springtime squall-line and dryline thunderstorm events in Oklahoma. They proposed that the orientation and movement of surface boundaries with respect to the deep-layer shear vectors might play a role in whether convection evolves linearly or remains discrete; similar to what was discovered in squall-line modeling studies by Weisman et al. (1988). Many questions remained unanswered, however. For instance, it was not clear whether lines evolved due to ''filling in'' spaces between cells via precipitation cascade, or if cold pools associated with original updrafts were the impetus for additional convective development in between existing cells.

Bluestein and Weisman (2000) discussed the dependence of the vertical shear profile orientation with respect to the initiating boundary on storm mode and evolution for numerically simulated supercells. They demonstrated that shear oriented normal to a line of forcing was associated with upscale linear growth through the interaction of splitting storm pairs at regular intervals along the line of forcing. On the other hand, shear oriented at an oblique angle to the boundary resulted in discrete cyclonic supercells, presumably given the propensity for the precipitation cascade to spread downstream with little interaction between adjacent storms or storm splits. Furthermore, Parker and Johnson (2000) noted that the orientation of the low-level forcing with respect to the environmental flow is significant in modulating the organization of the precipitation distribution associated with radar-observed linear mesoscale convective systems. They found that cold pool strength and longevity also appear to play an important role in convective organization. For a detailed discussion of cold pool evolution and its association to vertical shear and mean wind, refer to Corfidi (2003). James et al. (2005) observed that discrete modes were favored in environments with weak low-level shear but substantial deep-layer shear in both the line-parallel and line-perpendicular directions. For linearly evolving systems (slablike ascent), the normal component of the low-level shear and parallel component of the deep-layer shear tended to be comparatively stronger. Using numerical models, they confirmed their observations that stronger deep-layer shear oriented along the line resulted in a more rapid transition into a continuous surface gust front and subsequent along-line precipitation. However, modeling results from Bluestein and Weisman (2000) indicated that moderate along-line wind shear plays a role in maintaining discrete cells.

Most of the above-mentioned studies primarily focused on modeling results to identify environmental conditions that may modulate the convective mode and evolution. There has yet to be a comprehensive observational study to investigate the thermodynamic or kinematic variables that contribute to whether convection is likely to evolve into a quasi-linear system or remain discrete within the first few hours after initiation. Because the convective mode often has a strong influence on the primary severe weather threat, it is of utmost importance for an operational forecaster to be able to accurately forecast the modes of deep convection. Therefore, the primary goal of this study is to investigate and highlight statistically significant environmental parameters that modulate the organization and longevity of convection that develops along synoptic boundaries, namely cold fronts, drylines, and prefrontal troughs.

Details regarding the data collection are presented in section 2. In section 3, kinematic and thermodynamic parameters that have previously been shown to affect the convective mode and evolution in numerical simulations are evaluated. Specific attention is given to how the boundary orientation relative to the cloud-layer wind and shear vectors modulate the convective mode. A discussion on the influence of forcing such as low-level convergence and boundary type on mode evolution is also presented in section 3. Section 4 examines some individual case studies; a summary and discussion are presented in section 5, with conclusions in section 6.

2. Data and methodology

This study includes severe weather events east of the Rocky Mountains from autumn of 2003 through the summer of 2007, resulting in a total of four winter, spring, summer, and fall seasons. Events were identified in which 1) surface-based thunderstorms initiated along a synoptic boundary; 2) the storms produced one or more reports of large hail, damaging wind, and/or tornadoes; and 3) the 0–6-km AGL vector wind difference was 15 m s^{-1} or greater. These criteria are meant to represent the storm environments when the convective mode may largely determine the primary severe thunderstorm hazards, such as damaging winds with strongly forced derechos in the cool season (Evans and Doswell 2001; Coniglio et al. 2004; Burke and Schultz 2004), or tornadoes and large hail with discrete supercells. Since

cases were chosen that characterize the supercell parameter space (0–6-km vertical wind difference greater than 15 m s^{-1}), embedded supercell structures were sometimes observed even after storms had evolved into a solid line. Storms were determined to be surface based when the base of the effective inflow layer (Thompson et al. 2007) reached the ground level in observed or Rapid Update Cycle (RUC; Benjamin et al. 2004) proximity soundings modified for proximity surface conditions. The data included observed or hourly RUC model proximity soundings (Thompson et al. 2003), radar base reflectivity, Geostationary Operational Environmental Satellite (GOES) visible and infrared satellite imagery, surface aviation routine weather report (METAR) observations, and objective three-dimensional analyses based on a combination of hourly RUC and observed surface data (Bothwell et al. 2002). The latter fields are a time-matched merge of surface data with RUC2 data at 25-hPa vertical increments. The type of initiating boundary (cold front, dryline, or prefrontal trough) was determined subjectively using a methodology similar to that advocated by Sanders and Doswell (1995). Warm fronts, which are often ana-frontal in nature, were not included in the database. Operational experience at the SPC suggests that surface-based squall-line cases along warm fronts are rarely observed, though storms can sometimes evolve into clusters or mesoscale convective complexes on the cool side of the front.

Case selection favored the spring and late autumn (80 cases combined; Fig. 1), when surface-based instability and strong 0–6-km shear were most often observed in tandem. Winter cases (8) were limited by the less frequent occurrence of surface-based instability, while summer cases (16) were limited by weaker 0–6-km shear. Most of the cases collected include events east of the Rocky Mountains but along and west of the Mississippi River (Fig. 2).

About 90% of the upper-air data used in this study were obtained from RUC model point forecast proximity soundings and about 10% from observed soundings. The reliance on RUC soundings is due to the low spatial and temporal resolutions of the observed soundings. In this study, the definition of a proximity sounding is one located within 75 km and 1 h of the storm's initiation. Thunderstorm initiation was determined by the first appearance of ≥35-dBZ radar reflectivity using regional mosaic images of reflectivity at 0.5° elevation.

In an attempt to isolate parameters that may show skill in discriminating between storms that evolve into lines versus storms that remain discrete within 3 h of initiation, several kinematic and thermodynamic parameters were investigated. Kinematic parameters examined included the following: mean convergence in the lowest 90 hPa, the surface–2-km and surface–6-km shear vectors, both the normal and parallel components of the 2–6- or 2–8-km shear and mean wind vectors, the difference between the boundary motion and the component of the cloud-layer mean wind normal to the boundary, the angles between the 2–6- or 2–8-km mean wind vectors and the boundaries, the components of the surface to level of free convection (LFC) shear vectors normal to the boundaries, and the angle between the surface to LFC mean wind vectors and the boundaries. The layers used in the shear and mean wind calculations (2–6 or 2–8 km) were dependent on the depth of the convective cloud. The 2–6-km layer was used when estimated maximum storm tops were at or below 9 km above ground level (AGL), and the 2–8-km layer was used when estimated storm tops were above 9 km AGL. Storm tops were approximated using the equilibrium level from the RUC or observed proximity soundings. The advective component of storm motion is dependent on the mean wind through the cloud layer (Corfidi 2003). The 2–6- and 2–8-km layers were chosen to represent approximately the lowest 70%–80% of the cloud depth where most of the mass is concentrated, and are layers within the storm believed to be important for the distribution of precipitation influenced by storm-relative flow and shear (Brooks et al. 1994). Mean wind convergence in the lowest 90-hPa layer was obtained from a General Meteorological Package (GEMPAK; DesJardins et al. 1991) objective analysis script that calculates the convergence incorporating hourly RUC and observed surface data.

Several thermodynamic variables were collected, including the lowest 100-hPa mixed-layer convective available potential energy (MLCAPE), 100-hPa mixed-layer convective inhibition (MLCIN), capping inversion strength, 100-hPa mixed-layer lifted condensation level (MLLCL) height, and 100-hPa mixed-layer level of free

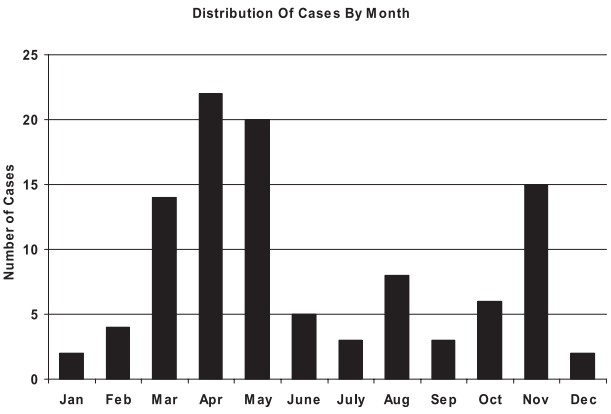

FIG. 1. Monthly distribution of convective mode cases from 2003 to 2007.

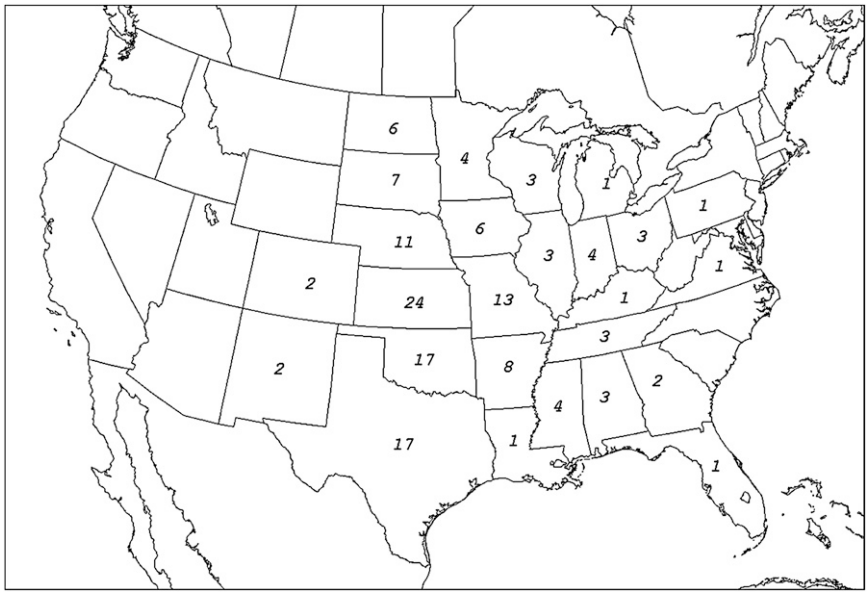

FIG. 2. Distribution of cases by state from 2003 to 2007.

convection (MLLFC), as well as the 1000–700- and 700–500-hPa layer-averaged relative humidities. If environmental parameters such as shear, MLCAPE, boundary orientation, etc., varied substantially within the region of concern, then the boundary was divided into multiple segments and each segment was considered as a separate case.

It must be emphasized that only storms thought to be initiated along a synoptic boundary were investigated in this study. The boundary was considered the initiation mechanism when storms developed within 40 km of its location. The average spacing between the surface observations varies, but 75 km is a good approximation for most locations east of the Rockies. One can be fairly certain of the location of a feature to within about half this spacing; therefore, a distance of 40 km was used to account for uncertainty in the boundary location. Storms were determined to move off the boundary when the distance between the boundary and the ≥35-dBZ reflectivity increased to more than 40 km. Deep convection that may have developed in the warm sector away from a synoptic boundary was not considered. Data from 105 cases were examined, including 39 events in which the storms remained discrete, 18 events in which mixed modes were observed, and 48 events in which storms evolved into lines—all within a 3-h time period. Storms were classified as lines when the contiguous ≥35-dBZ reflectivity pattern showed a length to width ratio of at least 5 to 1 (Fig. 3a). Storms were considered discrete when the maximum reflectivity between identifiable cells did not exceed 25 dBZ (Fig. 3b). Mixed modes were defined as a hybrid of discrete cells and line segments (Fig. 3c).

3. Results

In this investigation, parameters that exhibited skill in discriminating between discrete and linear evolutions were the ground-relative normal component of the mean cloud-layer wind, the normal component of the cloud-layer shear, the lowest 90-hPa layer convergence along the boundary, the type of initiating boundary, and the boundary-relative normal component of the mean cloud-layer wind. Among the kinematic parameters, the best skill was demonstrated by the boundary-relative normal component of the mean cloud-layer wind followed by the normal component of the cloud-layer shear.

a. Mean cloud-layer wind and vertical shear

Statistical results suggest that the ground-relative normal component of the mean wind through 70%–80% of the cloud-bearing layer (hereafter referred to as the normal component of the mean cloud-layer wind) can influence the short-term convective mode evolution. Figure 4a depicts a standard box-and-whiskers plot representing the component of the mean wind normal to the boundary at the time of initiation for storms that evolved into predominantly linear, mixed, and discrete modes at 3 h. Figure 4a indicates that a small overlap exists between the 75th percentile for lines and the 25th percentiles for cells. Lines and mixed modes, however, occupy a similar parameter space. To determine the

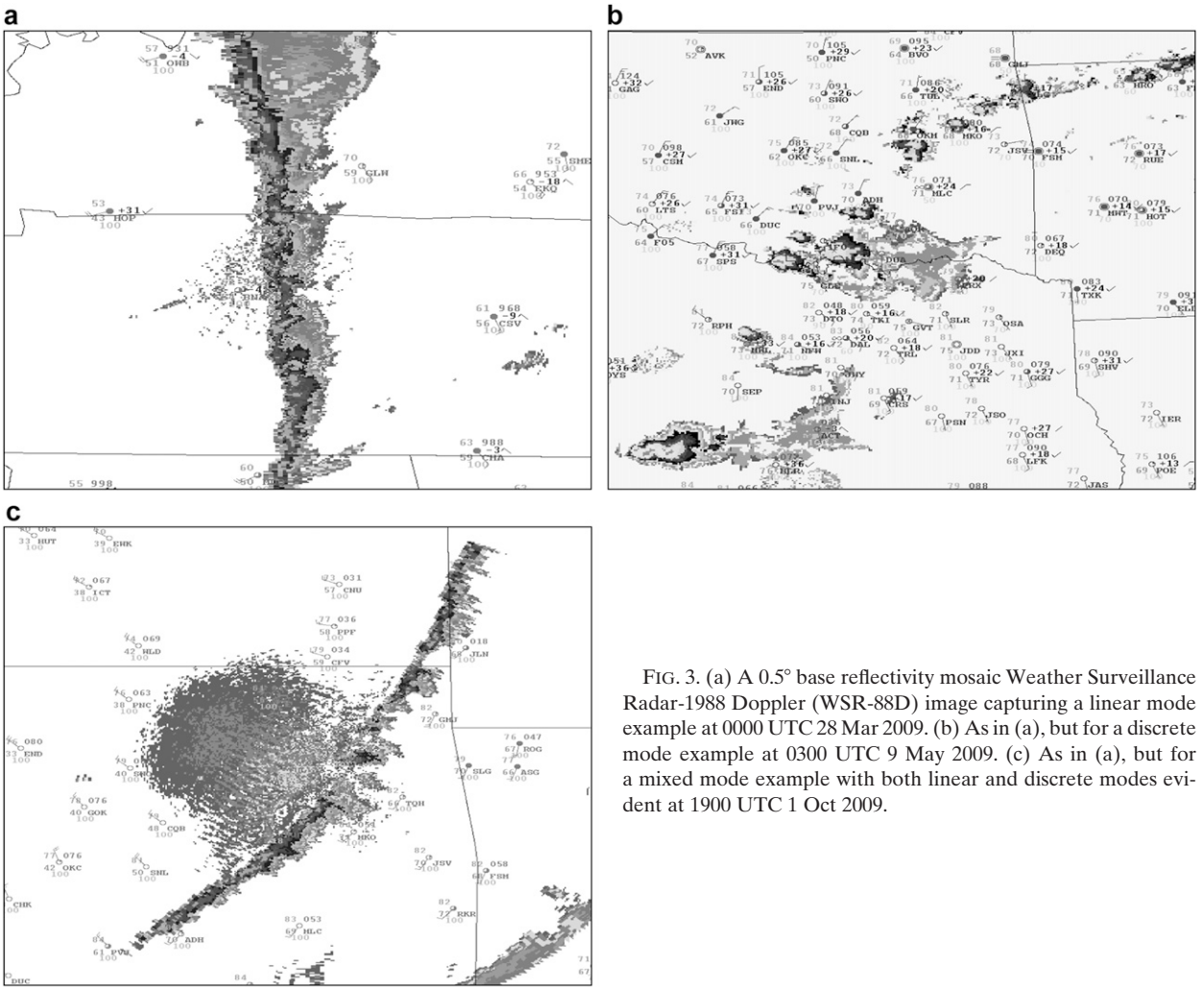

FIG. 3. (a) A 0.5° base reflectivity mosaic Weather Surveillance Radar-1988 Doppler (WSR-88D) image capturing a linear mode example at 0000 UTC 28 Mar 2009. (b) As in (a), but for a discrete mode example at 0300 UTC 9 May 2009. (c) As in (a), but for a mixed mode example with both linear and discrete modes evident at 1900 UTC 1 Oct 2009.

value of the normal mean cloud-layer wind component that best discriminates between linear and discrete modes, the threshold of the normal mean wind component was varied and a true skill score (TSS) was calculated for each value to yield a maximum TSS of 0.47, which corresponds to a mean wind of 10.5 m s^{-1}. The TSS is the difference between the probability of detection (POD) and the probability of false detection (POFD) and can be interpreted as the sum of the accuracy for events and the accuracy for nonevents. These results suggest that a small (less than 10.5 m s^{-1}) component of the mean cloud-layer wind normal to the initiating boundary supports faster evolution into linear modes and values greater than 10.5 m s^{-1} favor persistent discrete modes. Since the parameter space for mixed and linear modes is similar, a small normal component of the cloud-layer flow does not preclude the possibility of discrete cells remaining within the line at 3 h after initiation. The median normal component for lines is 8.5 versus 14 m s^{-1} for discrete cells. To quantify the significance of these results, the nonparametric Mann–Whitney test (Mann and Whitney 1947) was applied to the mean of the distribution to calculate a standard score of ± 4.4 and a p value of 1.09×10^{-5}, indicating the difference in the means is significant above the 99% confidence level.

The previous results include storms initiated by all boundary types in the database. Since mode evolution is determined in part by the nature of the initiating boundary, it is desirable to remove the variability of boundary type when computing the statistical significance of the influence of the cloud-layer mean wind on mode evolution (Fig. 4b). Results for storms that developed along prefrontal troughs are similar to those computed for all boundary types with a transition to linear modes favored when the normal component of the cloud-layer mean wind was less than 10 m s^{-1} and cells favored when the component exceeded 10 m s^{-1} based on a maximum TSS of 0.68. Results were also calculated for storms that

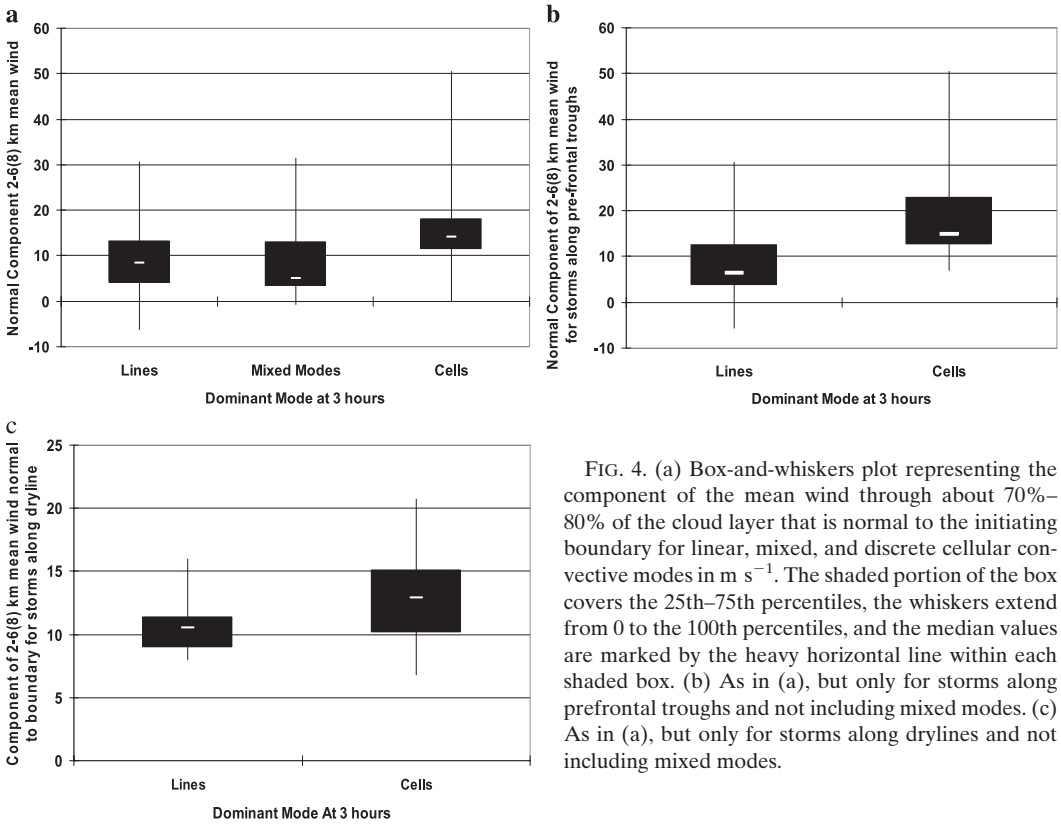

FIG. 4. (a) Box-and-whiskers plot representing the component of the mean wind through about 70%–80% of the cloud layer that is normal to the initiating boundary for linear, mixed, and discrete cellular convective modes in m s^{-1}. The shaded portion of the box covers the 25th–75th percentiles, the whiskers extend from 0 to the 100th percentiles, and the median values are marked by the heavy horizontal line within each shaded box. (b) As in (a), but only for storms along prefrontal troughs and not including mixed modes. (c) As in (a), but only for storms along drylines and not including mixed modes.

developed along drylines (Fig. 4c) with a transition to linear modes favored for normal components less than 12 m s^{-1}. However, the sample size for linear dryline cases was relatively small, and the sample size for discrete cold front cases was too small to compute statistical results.

The box-and-whiskers diagram for the normal component of the cloud-layer shear (Fig. 5a) indicates only a small overlap between the 75th percentile for lines and the 25th percentile for discrete cells. More specifically, lines are favored when the normal component is less than 8 m s^{-1} (based on a maximum TSS of 0.5) and persistent discrete cells are increasingly likely when the normal component exceeds 8 m s^{-1}. The Mann–Whitney test performed on these data indicates the difference in the means is significant above the 99% confidence level.

To isolate the influence of the normal component of shear on the mode from the variability of forcing related to the boundary type, this quantity was computed only for storms that developed along a prefrontal trough (Fig. 5b). Results were similar to those obtained when the normal component of the shear was computed for all boundary types with a transition to lines more likely when this quantity is less than 8 m s^{-1} and persistent discrete cells favored for values greater than 8 m s^{-1} based on maximum TSS value of 0.5.

Vertical shear in the 0–6-km layer is often used to discriminate between supercell and multicell environments. Modeling and observational studies have shown that a 0–6-km vector wind difference of less than 15 m s^{-1} supports multicell storms and values greater than 15 m s^{-1} are favorable for supercells given sufficient instability. However, upscale linear growth is sometimes observed in strong shear environments that would otherwise favor discrete supercells. It is therefore desirable to determine the parameter space of the 0–6-km vector wind difference and boundary orientation that best discriminates between linear and discrete modes. The box-and-whiskers diagram for the component of the 0–6-km vector wind difference normal to the initiating boundary (Fig. 5c) indicates a median shear of 12 m s^{-1} for storms that evolve into lines and 21 m s^{-1} for storms that persist as discrete supercells. Lines are favored for normal components of less than 15 m s^{-1} and discrete supercells are likely for normal components greater than 15 m s^{-1} based on a maximum TSS of 0.5. These results are consistent with modeling studies by Weisman et al. (1988), which suggest that storms initiated along a linear zone of forcing have an increasing tendency to develop three-dimensional supercell structures as the normal component of the 0–5-km shear is increased above

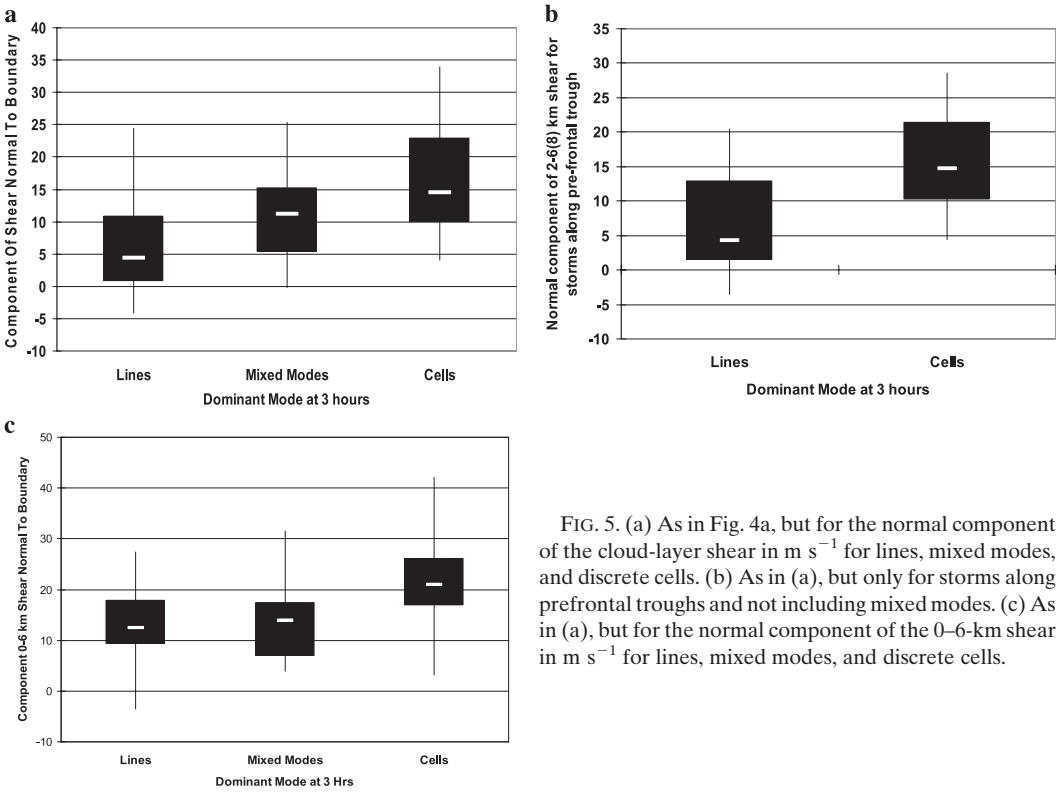

FIG. 5. (a) As in Fig. 4a, but for the normal component of the cloud-layer shear in m s^{-1} for lines, mixed modes, and discrete cells. (b) As in (a), but only for storms along prefrontal troughs and not including mixed modes. (c) As in (a), but for the normal component of the 0–6-km shear in m s^{-1} for lines, mixed modes, and discrete cells.

20 m s^{-1}. It should be reemphasized that since cases were chosen where the 0–6-km vector wind difference was within the supercell parameter space or greater than 15 m s^{-1}, embedded supercell structures were sometimes observed, even after storms had evolved into a solid line.

The relative magnitudes of the cloud-layer shear components normal and parallel to the initiating boundary were computed for linear and discrete evolutions (Fig. 6). It should be noted that for the parallel shear component, the absolute value was plotted since it should not matter which direction along the initiating boundary the parallel shear is directed. For linear evolutions, the data are skewed toward weaker normal components of shear. For persistent discrete evolutions, the data are skewed toward stronger normal shear components. Note that the parallel shear component does not appear to discriminate between mode types.

When forecasting linear modes, it is useful to know whether or not the convection will develop a trailing stratiform region (TSR), since observational evidence suggests that squall lines with TSRs are more likely to persist as lines and less prone to break up into discrete elements than lines that do not have a TSR. Parker and Johnson (2000) found that the distribution of stratiform precipitation within a mesoscale convective system (MCS) is related to the normal component of the storm-relative mean wind within the middle and upper levels of the atmosphere. They found MCSs that developed a TSR tended to form in environments with middle- to upper-level storm-relative flow directed toward the rear of the MCS. Later work by Parker and Johnson (2004a,b) indicated that the distribution of stratiform precipitation within an MCS is related to the normal component of deep-layer vertical shear.

In the current study, an attempt was made to differentiate between lines that developed a TSR within 3 h of initiation and those that did not develop a TSR. The normal component of the cloud-layer shear was found to be a statistically significant discriminator. The median normal component of the shear was 1.5 m s^{-1} for lines that developed a TSR and 7 m s^{-1} for lines that did not develop a TSR within this time (Fig. 7). A maximum TSS was achieved for a normal component of the cloud layer shear of 3.5 m s^{-1}. These results suggest that a small normal component of the shear (less than 3.5 m s^{-1}) may support faster development of a TSR due to the more rapid upstream distribution of hydrometeors.

b. Low-level convergence

The mean convergence in the lowest 90 hPa was used as a proxy for vertical motion along the boundary. In general, vertical motion within the first few kilometers above the surface should be proportional to the magnitude of the low-level convergence. Deep sustained

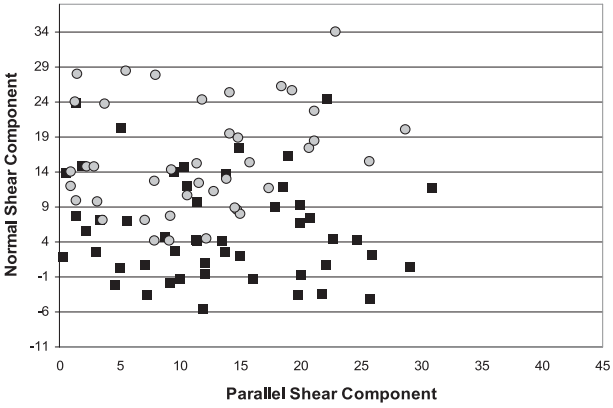

FIG. 6. Scatterplot of the component of cloud-layer shear normal to the boundary in m s^{-1} and the absolute value of the parallel shear component in m s^{-1} for cells (gray circles) and lines (black squares).

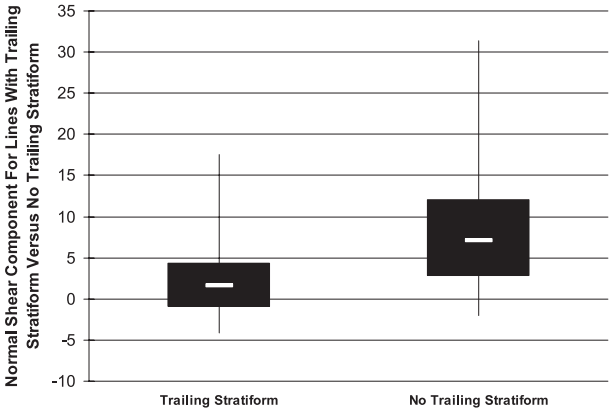

FIG. 7. As in Fig. 4a, but for the normal component of the shear in m s^{-1} for lines that developed a TSR within the first 3 h and for those that did not develop a TSR.

upward vertical motion can serve to weaken or eliminate convective inhibition associated with capping inversions and subsequently increase the likelihood of parcels reaching their LFC. The box-and-whiskers diagram (Fig. 8) indicates that a higher frequency of cases in which storms remained discrete within 3 h originated in environments with weaker low-level convergence than storms that quickly evolved into lines within this time. The difference in the means was determined to be significant at the 99% level using the Mann–Whitney significance test. The TSS of 0.3 was maximized at 8×10^{-5} s^{-1}, indicating a greater frequency of cases when storms evolved into lines within 3 h occurred in environments in which the initial low-level convergence was greater than 8×10^{-5} s^{-1}. In contrast, convergence values of less than 8×10^{-5} s^{-1} resulted in a greater frequency of persistent, discrete storms. Very rapid upscale linear growth is frequently observed within the zone of strong convergence and mesoscale ascent resulting from a cold front merging with a dryline. This process is best observed using high temporal and spatial resolution radar data as the merging of two fine lines. The magnitude of convergence associated with the merger will often be significantly underestimated, since it occurs on scales too small to be adequately sampled by most surface observation networks.

In our dataset, cold fronts were associated with higher values of low-level convergence with a median of 10×10^{-5} s^{-1} versus 6×10^{-5} s^{-1} for both prefrontal troughs and drylines. However, there are limitations to the computation of the convergence (Banacos and Schultz 2005) including scale dependence (our computational results are based on 40-km grid resolution, and higher grid resolutions would likely yield correspondingly larger values of convergence), uncertainty about the accuracy of the RUC analysis within the lowest 90 hPa above the surface, and the fact that low-level convergence is not always indicative of ascent through a deep layer of the atmosphere (Stensrud and Maddox 1988).

c. *Type of initiating boundary*

Results from this dataset suggest that prefrontal troughs and especially drylines have a tendency to produce persistent discrete modes more often than cold fronts, which are more frequently associated with convective lines (Fig. 9). Drylines are often characterized by a large component of westerly or southwesterly midlevel flow off the higher terrain of the Rockies or the Mexican plateau, which can result in a drier, warmer, and more capped midlevel environment due to the eastward advection of the elevated mixed layer (Lanicci and Warner 1991). Moreover, unlike slab ascent (Bryan and Fritsch 2000; James et al. 2005) frequently associated with cold fronts, the lift along a dryline is confined to a narrow zone with localized areas of enhanced low-level convergence. The often large westerly component of the middle-level flow and narrow zone of ascent can result in shorter updraft residence times within the region of mesoscale lift along the dryline (Ziegler and Rasmussen 1998). In addition, the proximity to elevated mixed layers often results in strong convective inhibition. These factors can decrease the chance for widespread initiation along the dryline and make isolated or widely scattered deep convective development more probable if deep-layer forcing is not sustained or strong enough.

The wedge of advancing cold air accompanying cold fronts frequently results in slablike ascent, especially from late fall through spring when fronts are generally stronger and the density discontinuity can be more pronounced, resulting in a higher frequency of linear evolution (Fig. 9). Slablike ascent typically associated

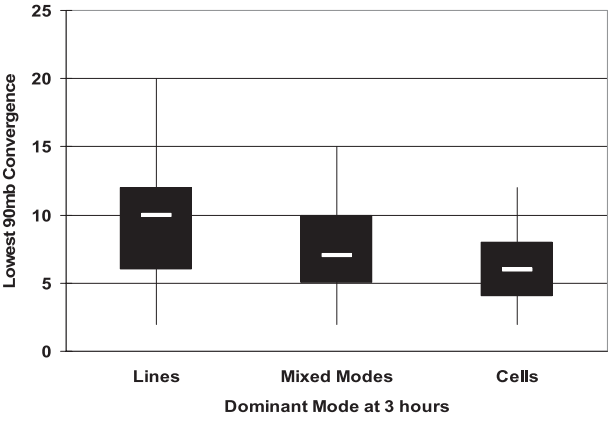

FIG. 8. As in Fig. 4a, but for the mean convergence in the lowest 90 hPa in 10^{-5} s^{-1} for lines, mixed modes, and discrete cells.

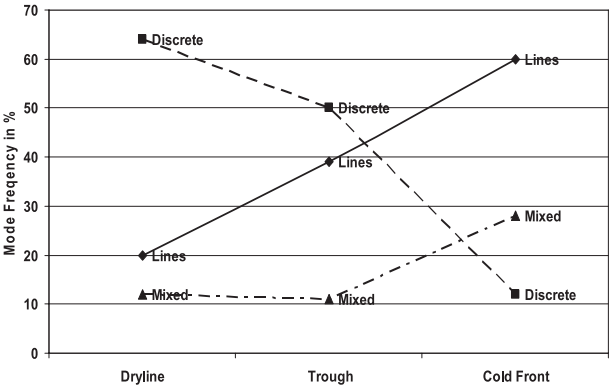

FIG. 9. Plot of mode frequency vs type of initiating boundary for drylines, prefrontal troughs, and cold fronts.

with cold fronts is more likely to result in the initiation of numerous storms as the front encounters lower static stability. Cold fronts are frequently associated with baroclinic midlatitude short-wave troughs of varying strengths and amplitudes that can promote sustained vertical motion through a relatively deep layer. These regions of sustained ascent also contribute to the removal or weakening of thermal inversions above the surface and are typically associated with less midlevel dry entrainment via layer lifting and moistening. Cold fronts accompanying higher-amplitude upper troughs are more likely to have a weaker normal component of mean wind and shear along much of its length, which can promote storms remaining within the zone of forcing along the boundary for longer periods of time.

d. Storm motion with respect to the initiating boundary

Three-dimensional numerical simulations by Jewett and Wilhelmson (2006) showed that storms evolve differently when initiated in environments where external mesoscale forcing is persistent and strong rather than weak. They found that a frontal circulation of modest intensity can have a lasting influence on a storm's morphology. Since the motion of a storm is due to both advection and propagation (Bunkers et al. 2000), the orientation of the mean cloud-layer wind vectors with respect to a boundary can have a significant influence, via advection, on the length of time developing updrafts remain near a boundary. In our dataset 82% of storms that did not move off the boundary evolved into lines or mixed modes within 3 h, and 77% of storms that moved off the boundary remained discrete within this time. It therefore appears that storms that remain within the zone of linear mesoscale convergence have a propensity to grow upscale at a faster rate.

Cloud-layer flow with a large component across the boundary often results in storms moving more rapidly away from the initial zone of lift, making persistent discrete modes more likely. Storms were determined to move off the boundary when the distance between the boundary and the 35-dBZ echo exceeded 40 km. However, a large normal component of cloud-layer flow does not guarantee that storms will move off the boundary since the speed of the boundary might also be faster in these environments and must be taken into account. A strong linear correlation between the boundary speed and the normal component of the mean cloud-layer wind is indicated (Fig. 10a) for environments when storms evolved into lines (0.75 correlation coefficient), and somewhat less so for those environments when storms remained discrete (0.63 correlation coefficient). The weaker correlation between the boundary speed and the mean wind in situations when storms remained discrete is due primarily to a greater number of dryline cases in which the dryline became stationary and subsequently retreated after the initiation of storms. Figure 10a shows that discrete modes were associated with a larger normal component of the mean cloud-layer wind relative to the speed of the boundary than were linear modes.

The boundary-relative normal component of the mean cloud-layer wind is a very good discriminator between when storms will move off the boundary and when storms will remain on the boundary (Fig. 10b). This parameter is also a very good discriminator for mode evolution (Fig. 10c). A maximum computed TSS of 0.75 corresponds to a boundary-relative normal-component of the mean cloud-layer wind of 6 m s^{-1}, indicating that discrete modes are likely for values greater than 6 m s^{-1} and the evolution to lines or mixed modes is likely for values less than 6 m s^{-1}. This parameter discriminates much better than simply using the ground-relative normal-component

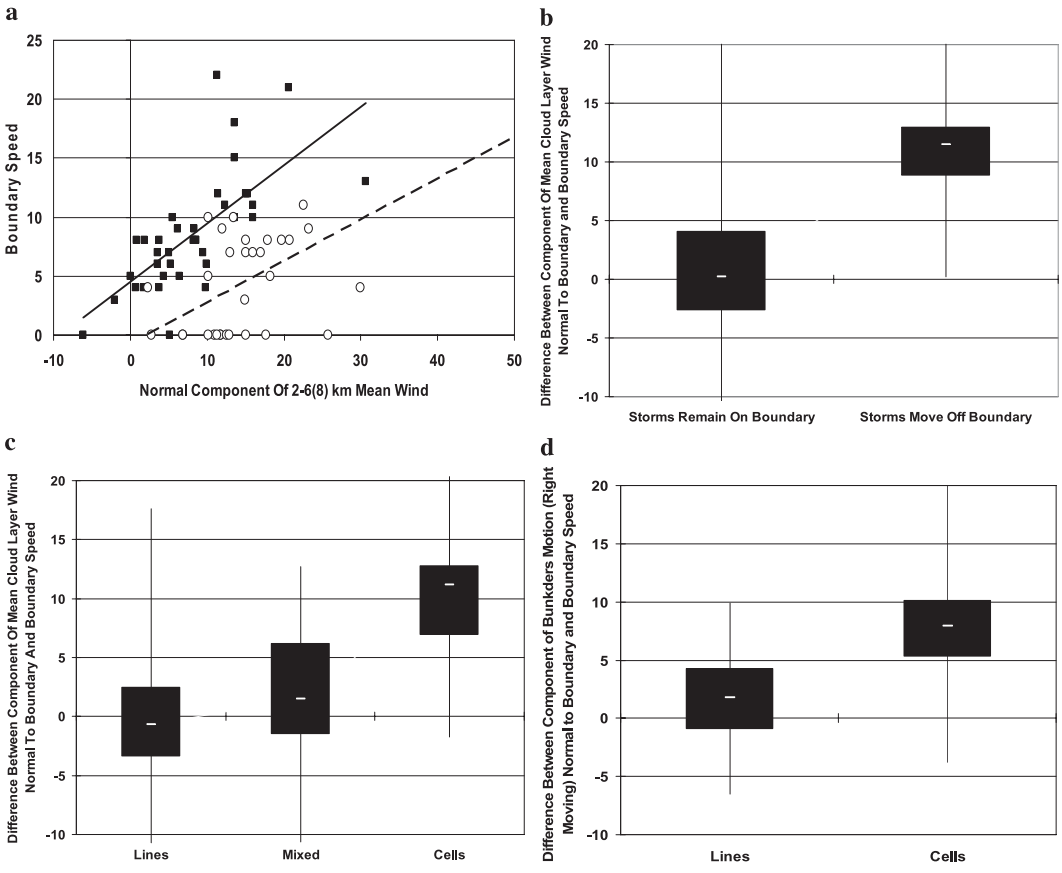

FIG. 10. (a) Scatterplot of the boundary speed vs the normal component of the cloud-layer mean wind in m s^{-1} for storms that evolved into lines (black squares) and storms that remained discrete (white circles). The trend line for linear cases is represented by the solid line, and the trend line for discrete cases is represented by the dashed line. (b) The boundary-relative normal component of the mean cloud-layer wind in m s^{-1} for storms that remain on the boundary within the first 3 h and those that move off the boundary within this time. (c) The boundary-relative, normal component of the mean cloud-layer wind in m s^{-1} for storms that evolved into lines and mixed modes, and those that remained discrete within 3 h after initiation. (d) The boundary-relative normal component of the Bunkers motion in m s^{-1} (right moving) for storms that evolved into lines and those that remained discrete within 3 h after initiation.

of the mean cloud-layer wind when evaluating the mode and whether or not storms will move away from the boundary.

Since storm motion is due to both the cloud-layer advective component and the propagation component, it was desirable to test a method that incorporates both components when estimating whether or not storms will move off a boundary and the effects on subsequent mode evolution. Our dataset only includes cases where the 0–6-km AGL vector wind difference was 15 m s^{-1} or greater, so a supercell motion technique (Bunkers et al. 2000) was used. Most hodographs in our dataset were characterized by veering wind profiles, favoring right-moving storms so the right-moving Bunkers motion was used. The Bunkers motion was preferred over the actual storm motion due to its prognostic value when utilized with point forecast soundings. The boundary-relative normal component of the Bunkers motion was calculated for storms that evolved into lines and those that remained discrete (Fig. 10d). The difference in the means was found to be statistically significant above the 99% level. A maximum TSS of 0.61 was computed that corresponds to a boundary-relative normal component of the Bunkers motion of 4.5 m s^{-1}, which is somewhat less than the TSS of 0.75 computed when using only the advective component. The lower discrimination potential when using the Bunkers motion is probably related to the assumption that all storms would evolve into supercells and move right of the mean shear vector. While a significant portion of the storms in our dataset did evolve into supercells, many storms never developed supercell characteristics.

Based on the results in this study, the authors believe that the boundary-relative normal component of the mean cloud-layer wind will usually suffice when estimating whether or not storms will move off the boundary. However, in situations where the boundary is quasi- stationary and the mean cloud-layer wind is nearly parallel to the boundary, the propagation component normal to the boundary could become large enough to result in storms moving away from the boundary. These situations would be considered a special case where the propagation vectors should be included when forecasting the normal component of the storm motion with respect to the boundary. If supercells are expected, the Bunkers motion can be used.

A plot of TSS versus parameter values (Fig. 11) indicates that the boundary-relative normal component of the mean cloud-layer wind is the best discriminator for the mode evolution of any kinematic parameter in our dataset (maximum TSS of 0.75) followed by the normal component of the cloud-layer shear with a maximum TSS of 0.52.

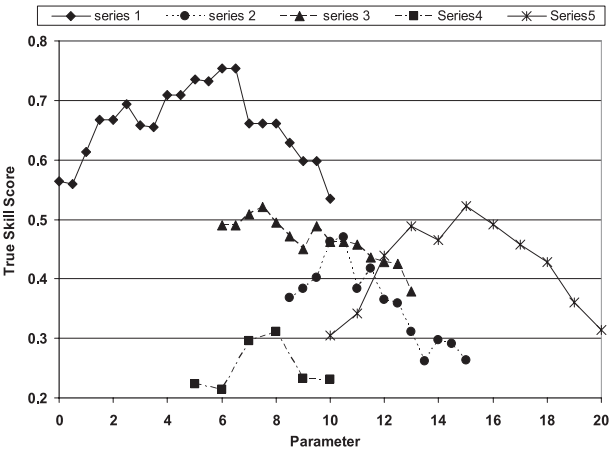

FIG. 11. Plot of TSS vs parameter values for the normal component of the mean cloud-layer wind relative to the speed of the boundary in m s^{-1} (series 1), the ground-relative normal component of the mean cloud-layer wind in m s^{-1} (series 2), the normal component of the cloud-layer shear in m s^{-1} (series 3), the mean lowest 90-hPa convergence in 10^{-5} s^{-1} (series 4), and the normal component of the 0–6-km shear in m s^{-1} (series 5).

e. Capping inversion or lid strength in warm sector

The mean of the inversion strength in the warm sector was calculated for environments when storms both remained discrete after moving off the boundary and evolved into lines within 3 h after moving off the boundary. The strength of the inversion was determined using the difference between the mean wet-bulb potential temperature in the moist boundary layer and the saturation wet-bulb potential temperature in the warmest part of the inversion. The mean inversion strength was determined to be 2.5°C for warm sectors when storms remained discrete after moving away from the boundary and 1.25°C when upscale linear growth occurred after storms moved off the boundary. However, it must be noted that the sample size for storms that evolved into lines within 3 h after moving away from the boundary was too small to compute statistical significance. For storms that remained on the boundary, the mean inversion strength was 2.3°C for discrete modes versus 1.6°C for storms that evolved into lines, but the difference in the means was not determined to be statistically significant.

4. Case study examples

a. 24 April 2007 (linear mode evolution)

On 24 April 2007, storms developed from northwestern Texas through western Oklahoma along a dryline (Fig. 12). Initial storms developed at 1530 UTC along this boundary and by 1730 UTC a dominant linear mode had evolved. Additional discrete storms developed in the warm sector, but our focus is only on the storms that formed along the dryline. The 500-hPa pattern was characterized by an upper low centered over southeastern Colorado and northeastern New Mexico, extending southward into western Texas. The boundary-relative normal component of the mean cloud-layer wind was slightly negative (-3.4 m s^{-1}), indicating that storms would remain within the zone of linear forcing. The cloud-layer shear vector was parallel to the dryline. A zone of low-level convergence of (8–12) $\times$ 10^{-5} s^{-1} was evident along the dryline, which appeared to be enhanced by the downward mixing of southwesterly momentum west of the moist axis. These values are in a range that would tend to promote an evolution to a linear or mixed mode. In this case, a small normal component of the mean cloud-layer wind with respect to the dryline allowed the storms to remain within the zone of linear forcing and appeared to play a significant role in the upscale growth to a dominant linear mode.

b. 26 August 2007 (persistent discrete modes)

On 26 August 2007, storms developed along a northeast–southwest-oriented prefrontal trough across eastern North Dakota (Fig. 13). Discrete supercell storms were the dominant mode during this episode, producing very large hail in excess of 2 in. and three significant tornadoes that resulted in one fatality and 13 injuries. Both the Advanced Research (ARW) and Nonhydrostatic Mesoscale Model (NMM) versions of the 4-km Weather

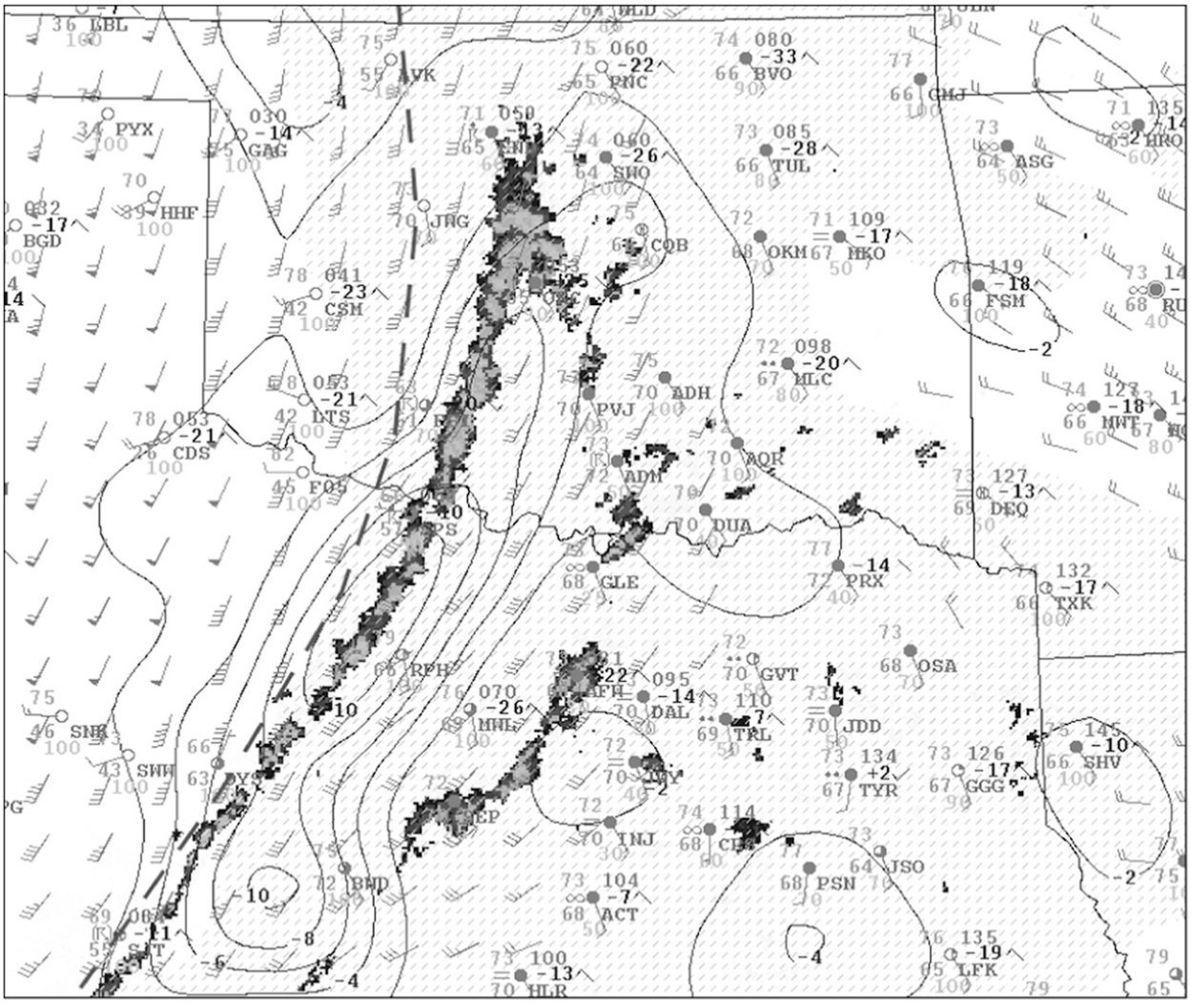

FIG. 12. Radar reflectivity (35 dB*Z* and above) for 1830 UTC 24 Apr 2007 with surface METARs, synoptic boundary locations, lowest 90-hPa mean convergence in 10^{-5} s^{-1} (solid lines), and 2–8-km AGL shear in kt (represented by the wind barbs).

Research and Forecasting Model (WRF) suggested that storms would develop and quickly evolve into dominant linear modes (not shown). Both of these models, however, initiated storms along the cold front farther to the northwest and not along the prefrontal trough, possibly suggesting a faster evolution to lines. In reality, the storms developed along the prefrontal trough in an environment with weak quasigeostrophic (QG) forcing and weak low-level convergence (4×10^{-5} s^{-1}). The boundary-relative normal component of the 2–8-km mean wind was 7 m s^{-1} and the motion of the storms relative to the speed of the trough was such that they moved off the boundary after initiation. The normal component of the shear was 8 m s^{-1}. These values, along with the weak linear convergence, are consistent with persistent discrete modes.

c. 21 April 2007 (squall line along cold front and discrete modes on dryline)

On 21 April 2007, storms developed along a cold front in west Texas and rapidly evolved into a squall line as the cold front merged with the dryline. To the east, however, initial storms developed along the dryline over west Texas. These storms remained discrete, producing several tornadoes and developed in an environment characterized by weak QG forcing. In contrast, storms that developed farther west along the cold front were in an environment consisting of strong low-level convergence, implying strong mesoscale ascent above the front (Fig. 14). Note that Fig. 14 does not show the dryline since by 0130 UTC the cold front had overtaken this feature. *Since the mean wind and cloud-layer shear orientations*

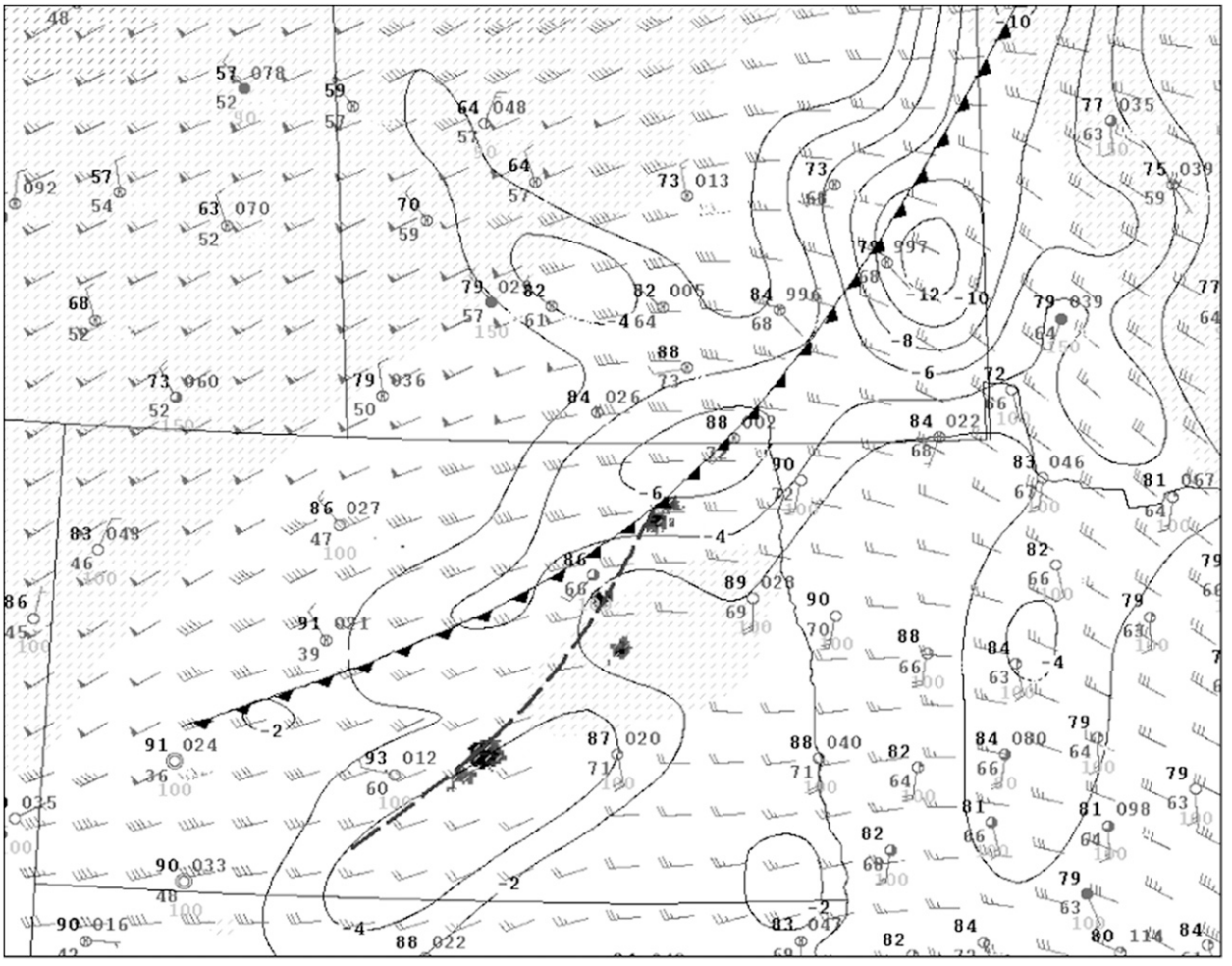

FIG. 13. As in Fig. 12, but for 2330 UTC 26 Aug 2007.

were essentially the same along both the dryline and cold front with large components directed across these boundaries, this case represents an example of how storms can evolve differently depending on the nature and magnitude of the external forcing, as well as the residence times of storms within the zone of forcing. The strong, linear forcing (low-level convergence 20×10^{-5} s^{-1} along the front) appeared to play a dominant role in the upscale evolution to lines as the front overtook the dryline. The relatively fast motion of the front (22 m s^{-1}) contributed to a boundary-relative normal component of the mean cloud-layer wind of -10.7 m s^{-1}, resulting in storms remaining within the zone of linear forcing despite a ground-relative cloud-layer wind component that would otherwise favor persistent discrete modes.

5. Summary and discussion

Results from this study indicate that the rate at which storms evolve into lines when initiated along a synoptic boundary is modulated primarily by the boundary-relative normal component of the mean cloud-layer wind, the nature and magnitude of the mesoscale forcing, and, secondarily, by the component of the cloud-layer shear normal to the boundary. The first determines the residence time of storms within the zone of forcing. It was found that when the difference between the normal component of the mean cloud-layer wind and the speed of the boundary is small, there is a tendency for storms to remain in the vicinity of the boundary with a faster rate of upscale linear growth (Fig. 15, example A). Mean boundary-relative cloud-layer wind with a large component normal to the boundary can promote storms moving more quickly away from the initial zone of lift, making persistent discrete modes more likely (Fig. 15, example B).

Once a line has formed, its longevity is strongly influenced by the ability to continually regenerate new updrafts along consolidated outflows of neighboring cells. The number of storms that develop is partly a function of

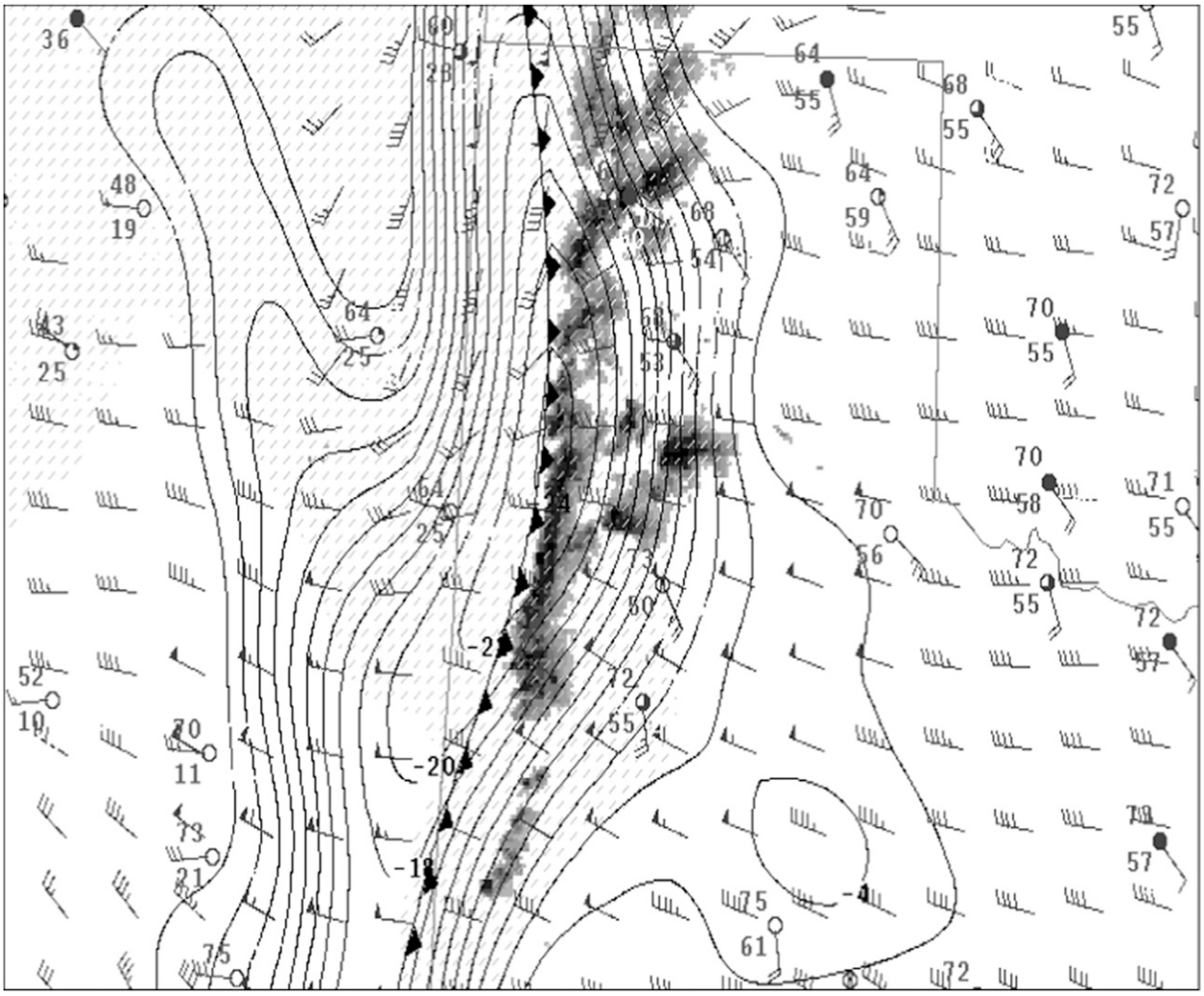

FIG. 14. As in Fig. 12, but for 0130 UTC 21 Apr 2007.

the magnitude and duration of deep mesoscale lift along the boundary. Deep, persistent mesoscale ascent can reduce the dry entrainment by moistening the thermodynamic profiles and can weaken or eliminate capping inversions, thereby making thunderstorm initiation more probable. In this study, mass convergence within the lowest 90 hPa was used as a proxy for vertical motion.

The distribution of precipitation and outflows with respect to the initiating boundary is largely determined by the orientation of the cloud-layer shear. This distribution appears to influence how efficiently precipitation cores can congeal and organize into a more solid line. Cloud-layer shear with a small component normal to the boundary can promote along-line or upstream distributions of hydrometeors, possibly contributing to a more rapid upscale linear growth. Conversely, a large normal component of the shear tends to favor persistent discrete storms.

Finally, it should be emphasized that this study is limited to the evolution of storms within a relatively short period after initiation due primarily to complicating factors associated with the potential for significant changes in the mesoscale environment as time progresses. Longer-term mode evolution is not addressed. However, even when environmental parameters initially support several hours of discrete modes, upscale growth to lines or clusters may eventually occur if enough storms develop and if storms persist long enough for their convective outflows to merge and consolidate.

With the possible exception of the capping inversion strength in the warm sector, which, along with the cold pool strength, likely play a role in whether or not storms will experience upscale linear growth after moving away from the initiating boundary, the thermodynamic parameters did not discriminate between types of short-term mode evolution in this research. The reason could

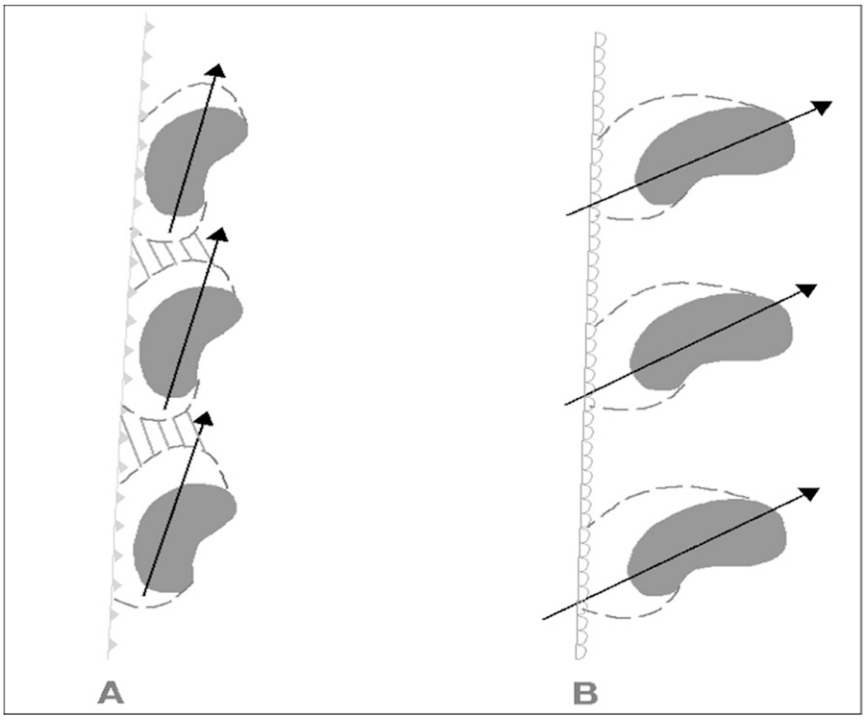

FIG. 15. Conceptual model showing the initiation of storms in two different flow regimes relative to the boundary. The dark arrows represent the mean cloud-layer wind and shear vector orientations, the shading represents precipitation regions, the dotted lines are convective outflow, and the hatched areas indicate where new development is likely as convective outflows merge.

be related to the representativeness of the RUC sounding data in areas where significant forcing is present. For example, in regions of mesoscale ascent and near boundaries where storms are developing, the thermodynamic environment is often in a state of transition, and it is difficult to determine a representative thermodynamic profile. The authors believe that quantities such as the strength of the capping inversion and the nature of the atmospheric moisture profiles do play a role in how storms evolve. For example, modeling work by French and Parker (2008) indicated that temperature perturbations within convective outflows were sensitive to changes in vertical moisture profiles. These perturbations, in addition to the amount of convective inhibition, can determine how effectively the outflows can generate new convection, which, in turn, would have an influence on future storm evolution.

6. Conclusions

Convective mode evolution is complex, involving many variables and processes that occur on the synoptic, meso-, and storm scales. Storms can evolve along outflow boundaries within the warm sector, along complex terrain features and synoptic boundaries, and in many combinations thereof. This paper establishes a connection between short-term (3 h) convective mode evolution and a few relevant parameters that can be diagnosed by the operational forecaster, but is limited to those situations in which storms developed along a synoptic boundary in environments containing both surface-based instability and vector wind differences > 15 m s^{-1} in the lowest 6 km.

Results from the Spring Experiments (Kain et al. 2008) that have been conducted at the NOAA Hazardous Weather Test Bed in Norman, Oklahoma, indicate that high-resolution numerical models, such as convection-resolving versions of the WRF, have often demonstrated skill in predicting how storms will evolve. It is desirable for the forecaster, however, to have an additional set of tools that can be used in conjunction with the high-resolution models to evaluate how storms might evolve within the first few hours of initiation. Results from this study indicate that, for storms initiated along a synoptic boundary, the residence time of storms within the zone of linear forcing, the nature and magnitude of linear forcing, and the normal component of the cloud-layer shear have a significant influence on the short-term mode evolution.

Storms that develop within a zone of strong, deep, linear forcing can experience rapid upscale growth into lines regardless of the orientation of the cloud-layer wind and shear vectors. Very rapid upscale linear growth is often

observed within the zone of enhanced convergence and mesoscale ascent resulting from a cold front merging with a dryline. A small boundary-relative normal component of the mean cloud-layer wind can promote storms remaining within the zone of linear forcing, which can accelerate upscale linear growth. Conversely, a large boundary-relative normal component of the mean cloud-layer wind directed toward the unstable warm sector can promote storms moving away from the initiation zone shortly after they develop. This scenario would tend to favor persistent discrete modes, but storm evolution would likely also depend on the nature and strength of the convective outflows and the capping inversion in the warm sector.

The authors have not attempted to address the influences of deep, large-scale forcing such as that associated with the upper jet and vorticity maxima in a quantitative sense. However, persistent deep-layer ascent that coincides with moderate to strong low-level convergence can modify the thermodynamic environment in such a way as to promote the development of numerous storms and a subsequent faster evolution to lines. The strength and location of upper-jet structures and their accompanying vorticity maxima relative to the surface boundaries likely play an important role in modulating the depth and magnitude of the upward vertical motion above the initiating boundary (Uccellini and Johnson 1979; Shapiro 1982).

Cursory observational evidence suggests that storms initiating in the warm sector away from discernible boundaries can often persist as discrete elements or a mix of discrete cells and multicellular cluster modes for many hours. In this study, however, no attempt has been made to investigate the relative frequency of discrete versus nondiscrete evolutions for warm sector initiation not associated with synoptic boundaries. Future research will focus on distinguishing between discrete and nondiscrete evolutions along outflow boundaries as well as in warm sectors when the initiating mechanisms are often subtle.

Acknowledgments. The authors would like to thank Steven Weiss (science and operations officer at the Storm Prediction Center), Matthew Parker, and the anonymous reviewers for their critical review of this paper. The authors would also like to thank Jason Levit (techniques development meteorologist at the Aviation Weather Center) for providing access to the data used in this study, and Harold Brooks of the National Severe Storms Laboratory for expert help with some of the statistical methods.

REFERENCES

Atkins, N. T., J. M. Arnott, R. W. Przybylinski, R. A. Wolf, and B. D. Ketcham, 2004: Vortex structure and evolution within bow echoes. Part I: Single-Doppler and damage analysis of the 29 June 1998 derecho. *Mon. Wea. Rev.,* **132,** 2224–2242.

Banacos, P. C., and D. M. Schultz, 2005: The use of moisture flux convergence in forecasting convective initiation: Historical and operational perspectives. *Wea Forecasting,* **20,** 351–366.

Benjamin, S. G., and Coauthors, 2004: An hourly assimilation–forecast cycle: The RUC. *Mon. Wea. Rev.,* **132,** 495–518.

Bluestein, H. B., and M. H. Jain, 1985: Formation of mesoscale lines of precipitation: Severe squall lines in Oklahoma during the spring. *J. Atmos. Sci.,* **42,** 1711–1732.

——, and S. S. Parker, 1993: Modes of isolated, severe convective storm formation along the dryline. *Mon. Wea. Rev.,* **121,** 1354–1372.

——, and M. L. Weisman, 2000: The interaction of numerically simulated supercells initiated along lines. *Mon. Wea. Rev.,* **128,** 3128–3149.

——, G. T. Max, and M. H. Jain, 1987: Formation of mesoscale lines of precipitation: Nonsevere squall lines in Oklahoma during the spring. *Mon. Wea. Rev.,* **115,** 2719–2727.

Bothwell, P. D., J. A. Hart, and R. L. Thompson, 2002: An integrated three-dimensional objective analysis scheme in use at the Storm Prediction Center. Preprints, *21st Conf. on Severe Local Storms/19th Conf. on Weather Analysis and Forecasting/15th Conf. on Numerical Weather Prediction,* San Antonio, TX, Amer. Meteor. Soc., JP3.1. [Available online at http://ams.confex.com/ams/pdfpapers/47482.pdf.]

Brooks, H. E., C. A. Doswell III, and R. B. Wilhelmson, 1994: The role of midtropospheric winds in the evolution and maintenance of low-level mesocyclones. *Mon. Wea. Rev.,* **122,** 126–136.

Bryan, G. H., and M. J. Fritsch, 2000: Moist absolute instability: The sixth static stability state. *Bull. Amer. Meteor. Soc.,* **81,** 1207–1230.

Bunkers, M. J., B. A. Klimowski, J. W. Zeitler, M. L. Weisman, and R. L. Thompson, 2000: Predicting supercell motion using a new hodograph technique. *Wea. Forecasting,* **15,** 61–79.

Burke, P. C., and D. M. Schultz, 2004: A 4-yr climatology of cold-season bow echoes over the continental United States. *Wea. Forecasting,* **19,** 1061–1074.

Coniglio, M. C., D. J. Stensrud, and M. B. Richman, 2004: An observational study of derecho-producing convective systems. *Wea. Forecasting,* **19,** 320–337.

Corfidi, S. F., 2003: Cold pools and MCS propagation: Forecasting the motion of downwind-developing MCSs. *Wea. Forecasting,* **18,** 997–1017.

Craven, J. P., and H. E. Brooks, 2004: Baseline climatology of sounding derived parameters associated with deep, moist convection. *Natl. Wea. Dig.,* **28,** 13–24.

DesJardins, M. L., K. F. Brill, and S. S. Schotz, 1991: GEMPAK 5. Part I—GEMPAK 5 programmer's guide. National Aeronautics and Space Administration, 4260 pp. [Available from Scientific and Technical Information Division, Goddard Space Flight Center, Greenbelt, MD 20771.]

Evans, J. S., and C. A. Doswell III, 2001: Examination of derecho environments using proximity soundings. *Wea. Forecasting,* **16,** 329–342.

French, A. J., and M. D. Parker, 2008: The initiation and evolution of multiple modes of convection within a meso-alpha-scale region. *Wea. Forecasting,* **23,** 1221–1252.

Funk, T. W., K. E. Darmofal, J. D. Kirkpatrick, V. L. DeWald, R. W. Przybylinski, G. K. Schmocker, and Y.-J. Lin, 1999: Storm reflectivity and mesocyclone evolution associated with the 15 April 1994 squall line over Kentucky and southern Indiana. *Wea. Forecasting,* **14,** 976–993.

Gallus, W. A., Jr., N. A. Snook, and E. V. Johnson, 2008: Spring and summer severe weather reports over the Midwest as a function of convective mode: A preliminary study. *Wea. Forecasting,* **23,** 101–113.

James, R. P., J. M. Fritsch, and P. M. Markowski, 2005: Environmental distinctions between cellular and slabular convective lines. *Mon. Wea. Rev.,* **133,** 2669–2691.

Jewett, B. F., and R. B. Wilhelmson, 2006: The role of forcing in cell morphology and evolution within midlatitude squall lines. *Mon. Wea. Rev.,* **134,** 3714–3734.

Kain, J. S., and Coauthors, 2008: Some practical considerations regarding horizontal resolution in the first generation of operational convection-allowing NWP. *Wea. Forecasting,* **23,** 931–952.

Lanicci, J. M., and T. T. Warner, 1991: A synoptic climatology of the elevated mixed-layer inversion over the southern Great Plains in spring. Part I: Structure, dynamics, and seasonal evolution. *Wea. Forecasting,* **6,** 181–226.

Mann, H. B., and D. R. Whitney, 1947: On a test of whether one of two random variables is stochastically larger than the other. *Ann. Math. Stat.,* **18,** 50–60.

Parker, M. D., and R. H. Johnson, 2000: Organizational modes of midlatitude mesoscale convective systems. *Mon. Wea. Rev.,* **128,** 3413–3436.

——, and ——, 2004a: Simulated convective lines with leading precipitation. Part I: Governing dynamics. *J. Atmos. Sci.,* **61,** 1637–1655.

——, and ——, 2004b: Simulated convective lines with leading precipitation. Part II: Evolution and maintenance. *J. Atmos. Sci.,* **61,** 1656–1673.

Przybylinski, R. W., 1995: The bow echo: Observations, numerical simulations, and severe weather detection methods. *Wea. Forecasting,* **10,** 203–218.

——, G. K. Schmocker, and Y.-J. Lin, 2000: A study of storm and vortex morphology during the intensifying stage of severe wind mesoscale convective systems. Preprints, *20th Conf. on Severe Local Storms,* Orlando, FL, Amer. Meteor. Soc., 173–176.

Rasmussen, E. N., and D. O. Blanchard, 1998: A baseline climatology of sounding-derived supercell and tornado forecast parameters. *Wea. Forecasting,* **13,** 1148–1164.

Sanders, F., and C. A. Doswell III, 1995: A case for detailed surface analysis. *Bull. Amer. Meteor. Soc.,* **76,** 506–521.

Shapiro, M. A., 1982: Mesoscale weather systems of the central United States. CIRES, University of Colorado/NOAA, Boulder, CO, 78 pp. [Available from Cooperative Institute for Research in Environmental Sciences, University of Colorado/NOAA, Boulder, CO 80309.]

Stensrud, D. J., and R. A. Maddox, 1988: Opposing mesoscale circulations: A case study. *Wea. Forecasting,* **3,** 189–204.

Thompson, R. L., R. Edwards, J. A. Hart, K. L. Elmore, and P. M. Markowski, 2003: Close proximity soundings within supercell environments obtained from the Rapid Update Cycle. *Wea. Forecasting,* **18,** 1243–1261.

——, C. M. Mead, and R. Edwards, 2007: Effective storm-relative helicity and bulk shear in supercell thunderstorm environments. *Wea. Forecasting,* **22,** 102–115.

Trapp, R. J., S. A. Tessendorf, E. S. Godfrey, and H. E. Brooks, 2005: Tornadoes from squall lines and bow echoes. Part I: Climatological distribution. *Wea. Forecasting,* **20,** 23–34.

Uccellini, L. W., and D. R. Johnson, 1979: The coupling of upper and lower tropospheric jet streaks and implications for the development of severe convective storms. *Mon. Wea. Rev.,* **107,** 682–703.

Weisman, M. L., and J. B. Klemp, 1982: The dependence of numerically simulated convective storms on vertical wind shear and buoyancy. *Mon. Wea. Rev.,* **110,** 504–520.

——, and ——, 1984: The structure and classification of numerically simulated convective storms in directionally varying wind shears. *Mon. Wea. Rev.,* **112,** 2479–2498.

——, ——, and R. Rotunno, 1988: Structure and evolution of numerically simulated squall lines. *J. Atmos. Sci.,* **45,** 1990–2013.

Ziegler, C. L., and E. N. Rasmussen, 1998: The initiation of moist convection at the dryline: Forecasting issues from a case study perspective. *Wea. Forecasting,* **13,** 1106–1131.